Research on the Application of Non-stationary Model in Analyzing the Evolution Law of Reference Evapotranspiration

Bin Gao[1], Baodeng Hou[1], Weihua Xiao[1,*], Xianglin Lyu[1], Hao Cui[1,2] and Wei Xue[1]
[1] *State Key Laboratory of Simulation and Regulation of Water Cycle in River Basin, China Institute of Water Resources and Hydropower Research, Beijing 100038, China*
[2] *College of Hydrology and Water Resources, Hohai University, Nanjing 210098, China*

Keywords: Reference evapotranspiration, Non-stationary, Penman-Monteith method, GAMLSS Model

Abstract: The Three Gorges Reservoir area (TGRA) is a typical ecological sensitive area in China. It is of great significance to clarify the non-stationary evolution law of evaporation under changing environment, which is the foundation to the study of water cycle, agricultural drought and irrigation etc. In this study, three models (Model 0, Model 1, Model 2) have been established to compare and analyze the non-stationary evolution laws and driving factors of reference evapotranspiration (ET_0) in TGRA. The results are as follows: (1) the annual ET_0 of stations with a ratio of ten twelfths shows a decreasing trend from -24.7 to -1.5 mm $(10a)^{-1}$; among them, the ET_0 of Badong, Zigui and Changshou stations decreased significantly ($P < 0.05$), and the decreasing amount was mainly contributed by autumn and summer; the significant decrease is caused by the combined effect of the decrease of sunshine hours (S), wind speed (U), relative humidity (RH) and the increase of average temperature (T), and the contribution rates of these factors are 80.38%, 48.32%, -23.21% and -5.48%, respectively. (2) The stationary model (Model 0) obviously is hard to explain the characteristics of ET_0 trend and mutation; the non-stationary model (Model 1) with time as the covariate can explain that the ET_0 sequence has a sudden change in 1979, and the ET_0 before and after the mutation point shows a sharp decline and a slow rise trend; even if the model fits well, the Model 1 lacks physical meaning and it is difficult to analyze the future evolution of ET_0; meteorological factors are used as covariates, the non-stationary model (Model 2) can better capture the distribution of ET_0 scattered points, and the AIC value is also significantly reduced, which verifies that the main contributors to the annual ET_0 change are S, U, which has certain physical significance.

1 INTRODUCTION

Evaporation is the main process of water and energy exchange in the water cycle. The actual evaporation is more helpful to the study of complex water circulation process, but the actual evaporation measurement is difficult, and cost is high, the method technology is difficult to be popularized comprehensively, the practicability is low, and the data accuracy is difficult to guarantee (Xing and He, 2021; Han et al., 2018). Therefore, the reference evapotranspiration (ET_0) is often used to estimate the surface evaporation in practice. ET_0 refers to the evaporation when the water supply condition of underlying surface is not limited. Its estimation methods include thomthwaite, Hamon, Hargreaves, Priestley Taylor, Penman-Monteith method, etc. Among them, the Penman-Monteith method revised by *FAO* in 1998 is widely used to estimate ET_0. It is based on the theory of energy balance and aerodynamics, considers the comprehensive influence of climate factors, and uses water vapor pressure, net solar radiation, wind speed and other factors to estimate ET_0, which has clear physical significance and is suitable for the calculation of ET_0 in different climate types (Li et al., 2016a).

Under the influence of climate change and human activities, it has become a consensus that there is non-stationary in hydrological time series, and the research results based on the stationary hypothesis have been questioned (Lu et al., 2020a). Trend and mutation test is the most used method to reflect the non-stationary characteristics of hydrological series. However, because the length of the sequence can directly affect the test results, and the length of the measured hydrological sequence

Gao, B., Hou, B., Xiao, W., Lyu, X., Cui, H. and Xue, W.
Research on the Application of Non-stationary Model in Analyzing the Evolution Law of Reference Evapotranspiration.
In *Proceedings of the 7th International Conference on Water Resource and Environment (WRE 2021)*, pages 28-36
ISBN: 978-989-758-560-9; ISSN: 1755-1315

generally ranges from several decades to one or two hundred years, which is far shorter than the complete hydrological process in the historical period of the watershed system, the representativeness of the hydrological sequence may not be sufficient (Xiong et al., 2015). Lu et al (2020b) pointed out that change does not mean non-stationary. Therefore, the non-stationary of hydrological series cannot be obtained simply based on the statistical test results, but also needs a clear hydrological process change to verify.

In this regard, some scholars (López and Francés, 2013; Zhang et al., 2015a; Zhang et al., 2015b; Lu et al., 2017) uses climate factors, meteorological factors, land use and other natural or human factors to simulate hydrological process change factors through generalized additive model (GAMLSS) and generalized extreme value model (GEV), so as to well reflect the non-stationary characteristics of hydrological series. The Three Gorges Reservoir area (TGRA) is a typical ecological sensitive area in China. It is of great significance to clarify the non-stationary evolution law of evaporation under changing environment, which is the foundation to the study of water cycle, agricultural drought and irrigation etc.

In this paper, the 12 stations daily meteorological data in TGRA from 1959 to 2019 are used to calculate the ET_0 by using the Penman-Monteith method. The spatial and temporal variation characteristics of the reference evapotranspiration are analyzed by using M-K method and ArcGIS spatial interpolation. The main factors affecting the non-stationary evolution of the ET_0 are quantitatively analyzed based on GAMLSS model and sensitivity analysis method, it provides theoretical guidance for the implementation of precision irrigation, efficient use of farmland water and optimal allocation of regional water resources in TGRA.

2 STUDY AREA AND DATA COLLECTION

2.1 Study Area

TGRA is located at the end of the upper reaches of the Yangtze River (28°10'~31°50'N, 105°10'~110°50'E), with an area of approximately 81,000 square kilometers (Figure 1). Its topography is characterized by deep valleys, rapid waters, vertical and horizontal ravines, broken mountains, frequent landslides, and a very fragile ecological environment (Ma et al., 2015). The reservoir area has a subtropical humid monsoon climate, with short winters and long summers, with annual rainfall ranging from 1000 to 1300 mm, abundant rainfall but uneven seasonal distribution. TGRA has a subtropical monsoon climate, and its annual average temperature is 17 ºC. Affected by atmospheric circulation and topography, the climate is unstable, there are many types of disastrous weather, and the frequency of floods and droughts is high, which seriously harms agricultural production (Liu et al., 2004).

2.2 Data Collection

This paper uses the daily data of 12 meteorological stations (Xingshan, Badong, Zigui, Zhenping, Fengjie, Wanzhou, Lichuan, Liangping, Changshou, Shapingba, Jiangjin, Hechuan) from 1959 to 2019, including the latitude and longitude of the stations, the data for altitude, maximum temperature, minimum temperature, average temperature, sunshine hours, relative vapor pressure and 2m high wind speed are all from the China Meteorological Science Data Sharing Network (http://data.cma.cn/).

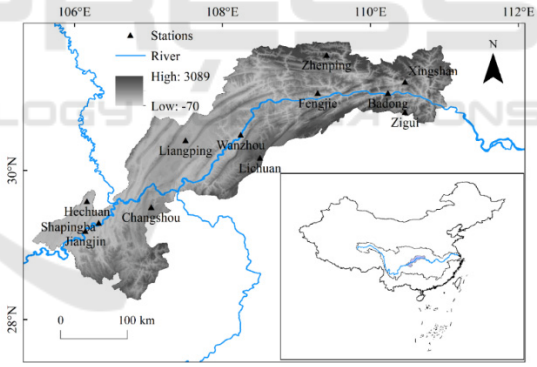

Figure 1: The location of the reservoir area and the distribution of meteorological stations.

3 METHODS

3.1 Penman-Monteith Method

This study is based on the Penman-Monteith method (Li et al., 2016b) revised by the Food and Agriculture Organization of the United Nations (FAO) in 1998 to estimate the ET_0 corresponding to the meteorological stations in TGRA. The calculation formula is as follows:

$$ET_0 = \frac{0.408\Delta(R_n - G) + \gamma \frac{900}{T+273} u_2 (e_s - e_a)}{\Delta + \gamma(1 + 0.34u_2)} \quad (1)$$

Where, Δ is the slope of the saturated vapor pressure curve (kPa · $^oC^{-1}$), R_n is the net solar radiation(MJ · m^{-2} · d^{-1}), G is the soil heat flux(MJ · m^{-2} · d^{-1}), γ is the psychrometric constant (kPa · $^oC^{-1}$), U is the wind speed (m · s^{-1}), T is the average temperature (^oC), e_s is the average saturated vapor pressure(kPa), e_a is the actual vapor pressure(kPa). The calculation process of R_n, e_s and e_a is detailed in literature (Bi et al., 2020).

3.2 Contribution Analysis based on Sensitivity

The sensitivity coefficient is defined by the ratio of ET_0 change rate to meteorological factor change rate, which is used to quantify the contribution rate of meteorological factors to ET_0 trend change (Zhang et al., 2019). The multiplication of the sensitivity coefficient of a single meteorological factor and its multi-year relative change rate is the contribution $con(x)$ of the meteorological factor to the change of ET_0, and the contribution of each meteorological factor is added to obtain the long-term trend of ET_0. In addition, the contribution rate of a single climate factor to the long-term trend of ET_0 is $p(x)$. If $p(x) > 0$, it means that the change of the factor has a promoting effect on the change of ET_0; if $p(x) < 0$, it means that the change of the factor has an inhibitory effect on the change of ET_0.

$$S_x = \lim_{\Delta x \to 0} \left(\frac{\Delta ET_0 / ET_0}{\Delta x / x} \right) = \frac{\partial ET_0}{\partial x} \times \frac{x}{ET_0} \quad (2)$$

$$con(x) = S_x \times \frac{n \cdot slope(x)}{\bar{x}} \quad (3)$$

$$\frac{dET_0}{ET_0} = con(S) + con(U) + con(RH) + con(T) \quad (4)$$

$$p(x) = \frac{con(x)}{\frac{dET_0}{ET_0}} \times 100\% \quad (5)$$

Where, x is a meteorological factor, $con(x)$ is the contribution of a meteorological factor to ET_0, slope(x) is the tendency rate of x, $\bar{x}$ is the average value of x in the period. x in this study refers to sunshine hours (S), wind speed (U), relative humidity (RH) and average temperature (T).

3.3 Generalized Additive Model based on Location, Scale and Shape Parameters

Generalized additive model based on location, scale, and shape parameters (GAMLSS) is a (semi) parametric regression model proposed by Rigby and Stasinopoulos (Stasinopoulos et al., 2008) in 2005 to analyze the non-stationary of series. It can flexibly use multiple distributions to describe the characteristics of random variable series, so as to establish the linear or nonlinear relationship between distribution parameters and covariates. Covariates can be time or physical factors.

3.3.1 Model Definition

It is assumed that the observed value y_t of random variable at time t obeys the probability density function $f(y_t|\theta^t)$, in which the distribution parameter θ^t can be reflected by the location parameter (θ_1) and scale parameter (θ_2). The mathematical description of the model is as follows:

$$g_k(\theta_k) = \eta_k = X_k \beta_k + \sum_{j=1}^{J_k} Z_{jk} \gamma_{jk} \quad (6)$$

Where, η_k is the observed value at time k, X_k is an explanatory variable matrix (which can be a time series or a function of meteorological factors), $g_k(\cdot)$ is a monotone differentiable connection function (which represents the functional relationship between θ_k and X_k), β_k is the J_k dimensional regression parameter vector (which can be expressed as $\beta_k^T = (\beta_{1k}, \beta_{2k}, \cdots, \beta_{J_k k})$), Z_{jk} and γ_{jk} are the j-th random effects.

Regardless of the influence of the random effect term, and the random variable obeys a two-parameter probability distribution, the general expression of the GAMLSS model can be expressed as:

$$g(\mu) = X_1 \beta_1 \quad (7)$$

$$g(\sigma) = X_2 \beta_2 \quad (8)$$

The likelihood function of GAMLSS model with regression parameter is as follows:

$$L(\beta_1,\beta_2)=\prod_{t=1}^{n} f(y_t\,|\beta_1,\beta_2) \quad (9)$$

Taking the maximum value of the likelihood function as the objective function, the RS algorithm (Stasinopoulos et al., 2008) can be used to estimate the optimal value of the regression parameters.

3.3.2 Model Construction

In this study, three models were constructed to compare the evolution characteristics of ET_0 (Table 1). When the distribution parameters are constant, it is the traditional stationary model (Model 0); When at least one distribution parameter changes with time t, it is a non-stationary model (Model 1). Model 1 has two fitting types, one is a linear function, the other is a parabolic function, and the optimal function fitting type is taken as the result of Model 1; When at least one distribution parameter is established as a function of meteorological factors, it is a non-stationary model (Model 2).

Log normal distribution and gamma distribution are selected to fit the annual maximum flow series of each station in TGRA, and the *AIC* value of each fitting is calculated. The smaller the *AIC* value is, the better the corresponding model is. Therefore, the annual maximum flow series is suitable for stationary or non-stationary models. After selecting the optimal fitting distribution by *AIC* value, the model fitting is further judged by the distribution characteristics of statistical model residuals.

$$GAIC=-2\ell(\hat{\theta})+\#\cdot df \quad (10)$$

Where, *GAIC* is the generalized *AIC* value, $\ell(\hat{\theta})$ is the log likelihood function corresponding to the estimated values of regression parameters, *df* is the degree of freedom of the model, # is the penalty factor (When # = 2, *GAIC* is *AIC* value).

Table 1: Model distribution parameters and combination of covariates.

Models	Schemes	θ_1 or θ_2
Model 0	1	ct
Model 1	2	$\beta_0+\beta_1 t$
	3	$\beta_0+\beta_1 t+\beta_2 t^2$
Model 2	4	$\beta_0+\beta_1 x_1$
	5	$\beta_0+\beta_1 x_1+\beta_2 x_2$
	6	$\beta_0+\beta_1 x_1+\beta_2 x_2+\beta_3 x_3$

4 RESULTS

4.1 Spatial Distribution Characteristics of *ET0*

The multi-year average ET_0 of TGRA is between 743.9 and 1000.5 mm, with an average of 864.3 mm (Figure 2e). From the upstream to the downstream of the reservoir area, ET_0 first decreases and then increases. The high-value areas are located in the Daba Mountain, Wushan, and Yangtze River Valley areas in the northeast of TGRA, and the low-value areas are located on the south side of the upper and middle reaches.

The four seasons and the annual ET_0 spatial distribution are generally similar, and there is a characteristic that high-value areas are located in the lower reaches. The range of ET_0 in spring is 195.9~270.0mm, and the low value area is on the south side of the middle and upper reaches (Figure 2a); the spatial range of ET_0 in summer is 307.1~396.8mm, and the low value area is in the mountain area on the south side of the middle reaches (Figure 2b); The range of ET_0 in autumn is 213.9~150.6mm, and the low-value area is in the main urban area of Chongqing (Figure 2c); the spatial range of ET_0 in winter is 75.3~132.3mm, and the low-value area is in the Yangtze River Valley in the middle reaches (Figure 2d). The order of the ET_0 value of each season is: summer>spring>autumn>winter, accounting for 42%, 27%, 20%, and 11% of the annual value, respectively. Among them, spring and summer contribute the most to the annual value, nearly 69%.

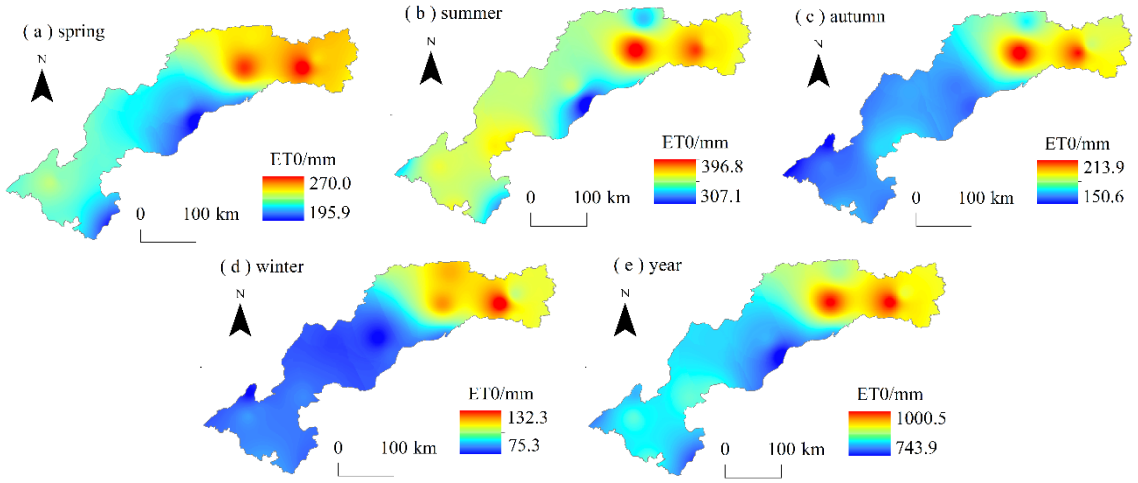

Figure 2: Spatial distribution of average *ET0*.

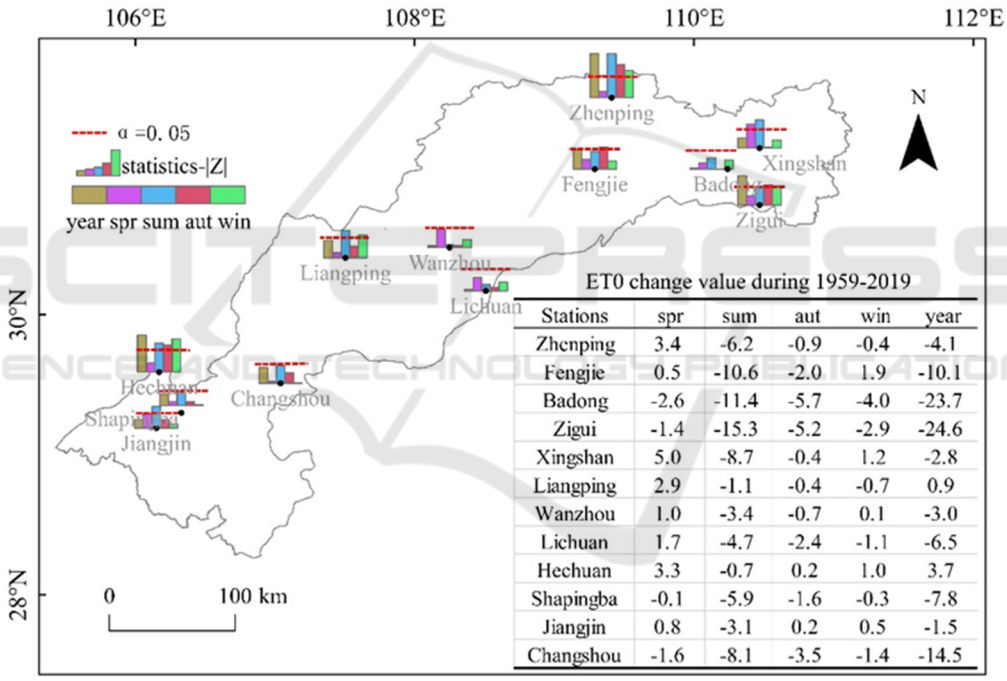

ET0 change value during 1959-2019

Stations	spr	sum	aut	win	year
Zhenping	3.4	-6.2	-0.9	-0.4	-4.1
Fengjie	0.5	-10.6	-2.0	1.9	-10.1
Badong	-2.6	-11.4	-5.7	-4.0	-23.7
Zigui	-1.4	-15.3	-5.2	-2.9	-24.6
Xingshan	5.0	-8.7	-0.4	1.2	-2.8
Liangping	2.9	-1.1	-0.4	-0.7	0.9
Wanzhou	1.0	-3.4	-0.7	0.1	-3.0
Lichuan	1.7	-4.7	-2.4	-1.1	-6.5
Hechuan	3.3	-0.7	0.2	1.0	3.7
Shapingba	-0.1	-5.9	-1.6	-0.3	-7.8
Jiangjin	0.8	-3.1	0.2	0.5	-1.5
Changshou	-1.6	-8.1	-3.5	-1.4	-14.5

Figure 3: MK test and spatial distribution characteristics of change values of ET_0 (mm $(10a)^{-1}$).

4.2 Seasonal Change Characteristics of ET_0

The annual and seasonal ET_0 trend test and the spatial distribution characteristics of the rate of change of the 12 stations in TGRA (Figure 3). The annual ET_0 has the Z value (MK's test statistics) of ten twelfths stations are negative, the change value is between -24.7~-1.5mm $(10a)^{-1}$ ($P < 0.05$). The significant decrease in annual ET_0 was mainly contributed by autumn and summer; the other two stations showed an insignificant increase trend, and the annual ET_0 change rate was 0.9 and 3.7mm $(10a)^{-1}$, respectively.

The ET_0 in the reservoir area showed an insignificant increase trend in spring, a significant decrease in summer ET_0 ($P < 0.05$), and an insignificant decrease trend in the ET_0 series in autumn and winter. The change rates of the four seasons were 1.1, -6.6, -1.9, -0.5mm $(10a)^{-1}$. According to the pettitt mutation test, ET_0 mutation occurred in 1979 in the year, summer and autumn (Figure 4).

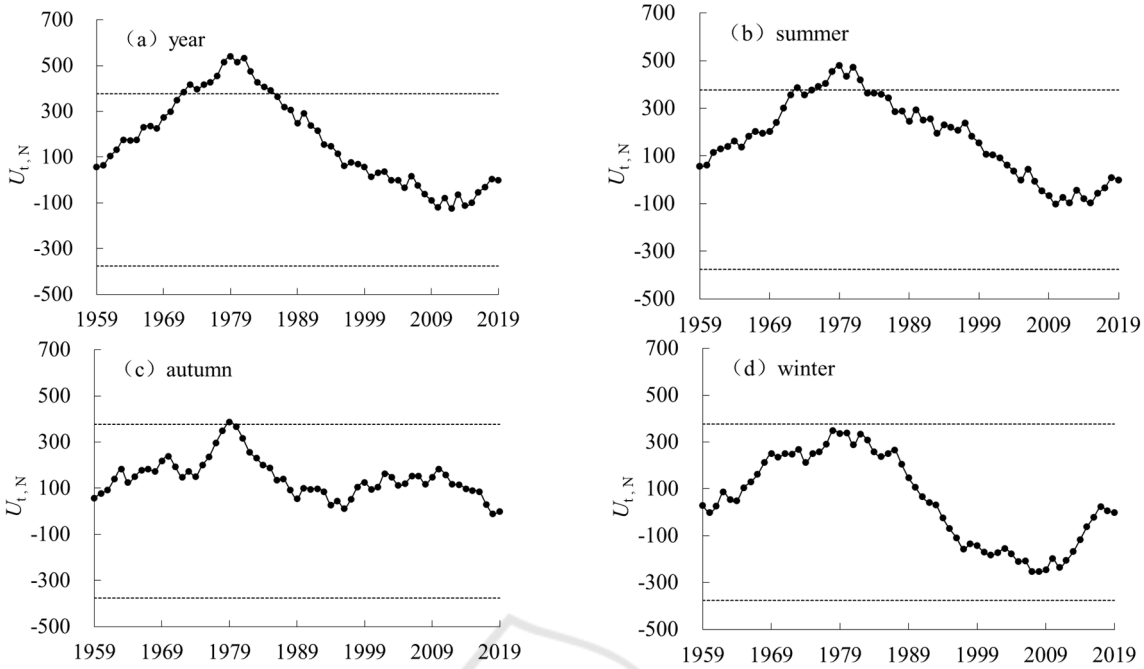

Figure 4: Annual and seasonal evaporation pettitt mutation test.

4.3 Driving Factor Analysis

Taking the seasonal mean values of *S*, *U*, *RH*, and *T* of the 12 stations in TGRA as representative values, the M-K test method is used to analyze the changing trends of the main meteorological factors in the four seasons, and the *Z* value of the statistics indicates a significant trend. The *k* value represents the tendency rate of the meteorological factor.

In the past 61 years, *S*, *U*, and *RH* in TGRA showed a decreasing trend (Table 2). Since the mid-1970s, the South Asian regional high and the western Pacific subtropical high have tended to shift to southwest China, and the East Asian monsoon has a weakening trend, which is not conducive to the production of wind and rain in southwest China (Tabari et al., 2013), and *T* is also increasing year by year, which has led to a downward trend in *RH* during the past 61 years, and a significant downward trend in *U* ($P < 0.01$ in spring, autumn and winter) (Liu et al., 2018); Yang Xiaomei studied the *S* in southwest China, which reveals that U is the main reason for the changes in *S*. The significant increase in *T* in TGRA ($P < 0.05$ in spring and autumn, $P<0.01$ in winter) is mainly due to the impact of global warming (Yang et al., 2012).

Table 2: M-K statistics and tendency rate of *ET0* and meteorological factor.

Series	Statistic	*S*	*U*	*RH*	*T*	ET_0
Spring	Z	0.351	-4.742*	-1.711	2.223**	0.572
	k	0.001	-0.005	-0.035	0.012	0.107
Summer	Z	-3.274*	-2.161**	0.353	-0.192	-2.201**
	k	-0.019	-0.002	0.003	-0.001	-0.660
Autumn	Z	-2.562*	-3.728*	-0.486	2.138**	-1.711
	k	-0.009	-0.003	-0.005	0.011	-0.185
Winter	Z	-1.213	-3.634*	-0.525	2.616*	-0.436
	k	-0.006	-0.004	-0.010	0.016	-0.050
Year	Z	-3.401*	-4.031*	-0.404	2.426**	-2.262**
	k	-0.008	-0.004	-0.013	0.009	-0.782

** indicate passing the 95% confidence test.*
*** indicate passing the 99% confidence test.*

Table 3: Contribution rate of meteorological factors to *ET0*.

Series	C(*S*)	C(*U*)	C(*RH*)	C(*T*)	C(ET_0)
Spring	62.01%	-311.00%	297.06%	51.92%	100.00%
Summer	88.65%	9.84%	1.38%	0.13%	100.00%
Autumn	71.79%	41.79%	-8.58%	-5.00%	100.00%
Winter	66.02%	86.85%	-30.91%	-21.96%	100.00%
Year	80.38%	48.32%	-23.21%	-5.48%	100.00%

Increasing (decreasing) of *S*, increasing (decreasing) of *U*, decreasing (increasing) of *RH*, and increasing (decreasing) of *T* will lead to an increase (decrease) of ET_0. The reason for the significant decrease in annual ET_0 in TGRA is caused by the combined effect of the decrease of *S*, *U*, *RH*, and the increase of *T*. The contribution rates of these factors are 80.38%, 48.32%, -23.21% and -5.48%, respectively. Obtained that the promotion effect of *RH* and *T* on ET_0 is less than the inhibitory effect of *S* and *U* on ET_0 (Table 3). Summer ET_0 shows a significant decreasing trend. The contribution rates of *S*, *U*, *RH* and *T* are 88.65%, 9.84%, 1.38% and 0.13%, respectively. The decreasing of *S*, the increase of *RH*, the decrease of temperature, and the decrease of wind speed all contribute to ET_0. Inhibition, so ET_0 showed a significant decreasing trend ($P < 0.05$); spring, autumn and winter will not be elaborated.

4.4 Non-stationary Evolution

The *AIC* criterion was used to analyze the fitting results of Model 0, Model 1, and Model 2 (Table 4). The best distribution of ET_0 in spring, autumn and winter is the Gamma distribution, and the best distribution of ET_0 in summer is the Normal distribution. Model 1 has a smaller *AIC* value than Model 0, that is, ET_0 in TGRA presents a non-stationary evolution law with time as a covariate. Compared with Model 0 and Model 1, when Model 2 uses meteorological factors as covariates to fit, the reduction of *AIC* value is significantly improved, indicating that the four seasons of the reservoir area ET_0 series all show non-stationary with meteorological factors as covariates. The following takes the annual scale as an example to analyze the inconsistent evolution law of the annual ET_0.

Table 4: Comparison of *AIC* values between the stationary model and the non-stationary model.

Series	Best distribution	Model 0	Model 1	Model 2
Spring	*GA*	547.4	547.1	411.8
Summer	*NO*	630.8	620.1	459.1
Autumn	*GA*	515.8	515.3	436.4
Winter	*GA*	430.1	418.1	368.5
Year	*GA*	668.1	654.5	593.9

GA—gamma distribution.
NO—normal distribution.

Table 5: Fitting residual distribution moments and Filliben coefficients of each model.

Series	Models	Mean	Variance	Skewness	Kurtosis	Filliben correlation
Spring	Model 0	0.00	1.0166	-0.0089	2.3731	0.9943
	Model 1	0.00	1.0166	-0.0490	2.3483	0.9939
	Model 2	0.00	1.0166	-0.0809	3.4609	0.9870
Summer	Model 0	0.00	1.0166	-0.0377	2.1356	0.9910
	Model 1	0.00	1.0166	0.1415	2.1060	0.9890
	Model 2	0.00	1.0166	0.2149	1.8555	0.9763
Autumn	Model 0	0.00	1.0166	0.2679	2.7754	0.9937
	Model 1	0.00	1.0166	0.2045	3.0307	0.9925
	Model 2	0.00	1.0166	-0.3125	3.1542	0.9913
Winter	Model 0	0.00	1.0166	0.2072	3.1358	0.9947
	Model 1	0.00	1.0166	0.0378	2.4756	0.9935
	Model 2	-0.01	1.0160	-0.0330	2.3311	0.9946
Year	Model 0	0.00	1.0166	0.0018	2.4222	0.9952
	Model 1	0.00	1.0166	0.3001	2.8050	0.9934
	Model 2	0.00	1.0166	0.2292	2.4102	0.9927

Quantile map of each model of annual ET_0 in TGRA (Figure 5). The stationary model (Model 0) cannot well capture the variation characteristics of ET_0 scatter points (Figure 5a); the non-stationary

model (Model 1) with time *t* as a covariate can well capture the time series distribution of ET_0 scatter points (Figure 5b), ET_0 showed a downward trend from 1959 to 1979, ET_0 showed an upward trend from 1980 to 2019, and 1979 was a mutation point, which is consistent with the results of the pettitt mutation test. However, the Model 1 cannot determine whether the annual ET_0 continues to increase after 2019, and the fitting result lacks physical meaning. The non-stationary model (Model 2) with meteorological factors as covariates captures the ET_0 scatter better than Model 1, and the *AIC* value is also significantly reduced, and has certain physical meaning (Figure 5c). With meteorological factors as the driving factor, the annual ET_0 dropped sharply from 1978 to 1981, and then the ET_0 showed an increasing trend in the following years.

The Filliben coefficients of the fitting residuals of each model are basically greater than 0.979, indicating that the residuals of each model obey the normal distribution well (Table 5).

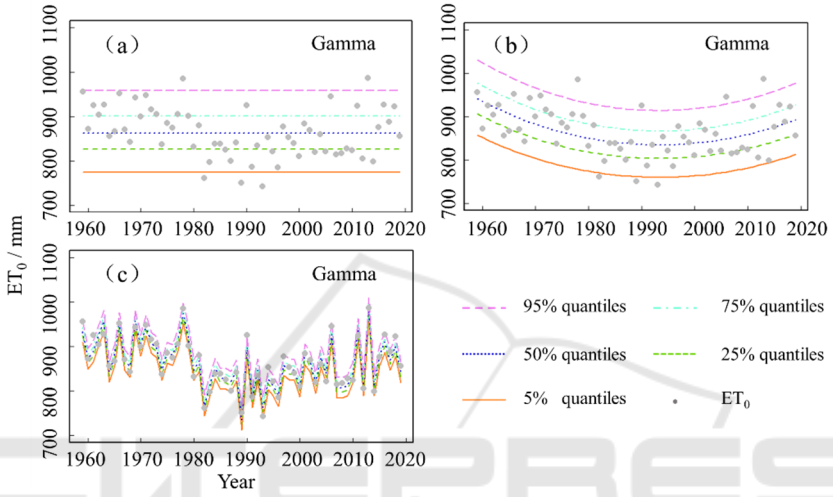

Figure 5: Comparison of quantiles diagrams between Model 0, Model 1 and Model 2.

5 CONCLUSIONS AND SUGGESTIONS

In the past 61 years, the annual ET_0 of ten twelfths stations has shown a decreasing trend by a linear regression analysis, and the rate of decrease is -24.7~-1.5mm $(10a)^{-1}$. Among them, the annual ET_0 of Badong, Zigui and Changshou stations has decreased significantly ($p<0.05$), the decrease is mainly contributed by the autumn and summer seasons. The annual and summer ET_0 decreased significantly ($p<0.05$). There was a mutation in ET_0 in the year, summer and autumn in 1979.

The contribution rates of S, U, RH and T for the significant decrease in annual ET_0 are 80.38%, 48.32%, -23.21% and -5.48% respectively, and the promotion effect of RH and T on ET_0 is less than the inhibitory effect of S and U on ET_0.

The stationary model (Model 0) obviously cannot explain the significant change trend and mutation characteristics of ET_0; the non-stationary model (Model 1) with time as a covariate can capture that the ET_0 sequence has a mutation in 1979, before and after the mutation point ET_0 is a steep decrease and a slow increase trend, respectively, explaining the characteristics of the significant change trend and sudden change of ET_0, but lacks certain physical meaning, and the future changes of ET_0 are difficult to predict; a non- stationary model with meteorological factors as covariates (Model 2) , It can better capture the distribution of ET_0 scattered points, and the *AIC* value is also significantly reduced, verifying that the main contributing factors that cause the annual ET_0 change are *S*, *U*, and *RH*, which have certain physical significance.

ACKNOWLEDGMENTS

The researchers would like to extend theirs thanks to the National Natural Science Foundation of China (No. 51779271) and National Key Research and Development Program of China (No. 2017YFC0404701).

REFERENCES

Bi, Y. J., Zhao, J., Zhao, Y., Xiao, W. H., & Meng, F. J. (2020). Spatial-temporal variation characteristics and attribution analysis of potential evapotranspiration in Beijing-Tianjin-Hebei region. *Transactions of the Chinese Society of Agricultural Engineering*, *36*(5), 130-140.

Han, H. Q., Bai, Y. M., & Zhang X. D. (2018). Study on applicabilities and modifications of several methods for estimating reference crop evapotranspiration in Guizhou Province. *Water Resources and Hydropower Engineering*, *49*(10), 198-204.

Liu, C. Z., Li, T. F., Wen, M. S., Wang, X. P., & Yang, B. (2004). Assessment and early warning on geo-hazards in the Three Gorges Reservoir region of Changjiang River. *Hydrogeology & Engineering Geology*, *4*(2), 9-19.

Liu, Y., Cui, N. B., Li, G., Luo, W. Q., Liao, G. L., & Wang, L. T. (2018). Attribution Analysis of Seasonal Reference Crop Evapotranspiration in Southwest China in Recent 56 Years. *Water Saving Irrigation*, *280*(12), 59-64.

Lu, F., Xiao, W. H., Yan, D. H., & Wang, H. (2017). Progresses on statistical modeling of non-stationary extreme sequences and its application in climate and hydrological change. *Journal of Hydraulic Engineering*, *48*(4), 379-389.

Lu, F., Xiao, W. H., Dai, Y. Y., & Song, X. X. (2020a). Research on non-stationary hydrological frequency calculation in the mainstream of the Yellow River. *Journal of Hydroelectric Engineering*, *221*(12), 76-84.

Lu, F., Song, X. Y., Xiao W. H., Zhu, K., & Xie, Z. B. (2020b). Detecting the impact of climate and reservoirs on extreme floods using nonstationary frequency models. *Stochastic environmental research and risk assessment*, *34*(1), 169-182.

López, J., & Francés F. (2013). Non-stationary flood frequency analysis in continental Spanish rivers, using climate and reservoir indices as external covariates. *Hydrology & Earth System Sciences*, *8*(17), 3189-3203.

Li, S. E., Kang, S. Z., Zhang, L., Zhang, J. H., Du, T. S., & Tong, L. (2016a). Evaluation of six potential evapotranspiration models for estimating crop potential and actual evapotranspiration in arid regions. *Journal of Hydrology*, *543*, 450-461.

Li, Y. Z., Liang, K., Bai, P., Feng, A. Q., Liu, L. F., & Dong, G. T. (2016b). The spatio-temporal variation of reference evapotranspiration and the contribution of its climatic factors in the Loess Plateau, China. *Environmental Earth Sciences*, *75*(4), 1-14.

Ma, J., Li, C. X., Wei, H., Ma, P., Yang, Y. J., Ren, Q. S., & Zhang, W. (2015). Dynamic evaluation of ecological vulnerability in the Three Gorges Reservoir Region in Chongqing Municipality, China. *Acta Ecologica Sinica*, *35*(21), 7117-7129.

Stasinopoulos, D. M., Rigby, R. A., & Akantziliotou, C. (2008). Instructions on how to use the GAMLSS package in R. *Accompanying documentation in the current GAMLSS help files*.

Tabari, H., Grismer, M. E., & Trajkovic, S. (2013). Comparative analysis of 31 reference evapotranspiration methods under humid conditions. *Irrigation Science*, *31*(2), 107-117.

Xiong, L. H., Jiang, C., Du, T., Guo, S. L., & Xu, C. Y. (2015). Review on Nonstationary Hydrological Frequency Analysis under Changing Environments. *Journal of Water Resources Research*, *4*(4), 310-319.

Xing, Y., & He, Z. H. (2021). Study on Characteristics and Driving Mechanism of Evapotranspiration of Reference Crops in Vegetation Growing Season in Karst Area, Taking Guizhou Province as an example. *Science Technology and Industry*, *21*(4), 264-272.

Yang, X. M., An, W. L., Zhang, W., Chang, L., & Wang, Y. M. (2012). Variation of sunshine hours and related forces in southwestern China. *Journal of Lanzhou University (Natural Sciences)*, *48*(5), 52-59.

Zhang, D. D., Yan, D. H., Wang, Y. C., Lu, F., & Liu S. H. (2015a). GAMLSS-based nonstationary modeling of extreme precipitation in Beijing–Tianjin–Hebei region of China. *Natural Hazards*, *77*(2), 1037–1053.

Zhang, Q., Gu, X. H., Singh, V. P., Xiao, M. Z., & Chen, X. H. (2015b). Evaluation of flood frequency under non-stationarity resulting from climate indices and reservoir indices in the East River basin, China. *Journal of Hydrology*, *527*, 565-575.

Zhang, P. F., Zhao, G. J., Mu, X. M., Gao, P., & Sun, W. Y. (2019). Spatiotemporal Variation and Driving Factors of Pan Evaporation in the Weihe River Basin. *Arid Zone Research*, *36*(4), 973-979.